

# FIVE YEARS AT THE MOVIES

N.W. EVANS<sup>1,2</sup> AND V. BELOKUROV<sup>2</sup>

<sup>1</sup> *Institute of Astronomy, Madingley Rd, Cambridge CB3 0HA*

<sup>2</sup> *Theoretical Physics, 1 Keble, Oxford OX1 3NP.*

Applications of the forthcoming *GAIA* satellite to the study of variable phenomena (microlensing and supernovae) are discussed.

## 1 Introduction

*GAIA* is an astrometric satellite which has recently been approved by the European Space Agency for launch in about 2010. It will measure the angles between objects in fields that are separated on the sky by about a radian. Data will stream continuously at 1 Mbps from *GAIA*'s three telescopes, providing information on the positions of the billion or more astrophysical objects brighter than 20th magnitude. The motion of objects across the sky, due to both their space motion and their parallactic motion and the variability in the brightnesses of objects in 15 wavebands will be measured because each object is observed at least 150 times during the 5 year mission lifetime. From the raw time series, a three-dimensional movie of the motions of stars in the Galaxy will be synthesized. Just as the human brain interprets signals from the retina in terms of moving three-dimensional objects, so *GAIA* will interpret signals from its sensors in terms of moving astrophysical objects. *GAIA*'s job is dramatically the more difficult because (1) *GAIA*'s sensors return time-series rather than images, (2) the global adjustment of the myriad of instantaneous positions is a computational task of huge complexity, (3) *GAIA* has to correct for gravity-induced distortions of space-time, and (4) *GAIA* sees in 15 colours rather than three.

This article presents highlights from the five-year *GAIA* movie show. The alert despatcher in the *GAIA* mission will provide forewarning of many kinds of bursting and variable phenomena. We discuss two applications in detail here. First, the astrometric microlensing signal will allow us to take a complete inventory of all objects – no matter how dark – in the solar neighbourhood. Second, the catalogue of supernova (SN) detections will be the largest ever taken. It will provide opportunities both for follow-ups in other wavebands and numerous examples of scarce phenomena (like SNe II-L or SNe Ib/c).

## 2 Dark Matter in the Solar Neighbourhood

There are many direct detection experiments searching for the particle dark matter in the solar neighbourhood [1]. A crucial question is: how much particle dark matter is there? This is not an easy question to answer. Within 1.1 kpc of the Galactic plane, the column density of all matter is  $\sim 71M_{\odot}\text{pc}^{-2}$ , of which  $\sim 41M_{\odot}\text{pc}^{-2}$  is already accounted for by the known populations of stars and gas [2]. This leaves  $\sim 30M_{\odot}\text{pc}^{-2}$  as the column density of dark matter. *How much of the missing matter is made up from elementary particles, as opposed to dark compact objects like dim stars?*

*GAIA* is the first instrument which has the capability of answering this question. Local populations of black holes and halo or disk white dwarfs could easily have eluded identification thus far. Similarly, there may be an extensive local population of very cool brown dwarfs. The *2 Micron All Sky Survey* and the *Sloan Digital Sky Survey* have increased the known population of local dwarf stars with spectral types later than M to over a hundred [3]. Nonetheless, the coolest brown dwarfs will have easily eluded the grasp of these and all current surveys. Future projects like the *Space Infrared Telescope Facility* may be able to detect very old brown dwarfs in the solar neighbourhood by using long integration times, but a large-scale survey will be prohibitively costly in terms of time. However, the astrometric microlensing signal seen by *GAIA* will be sensitive to local populations of even the dimmest of stars and darkest of these objects.

*GAIA* cannot resolve the two images of a microlensed source. However, *GAIA* can measure the small deviation (of the order of a fraction of a milliarcsec) of the centroid of the two images around the trajectory of the source. Astrometric microlensing is the name given to this excursion of the image centroid [4]. The cross section of a lens is proportional to the area it sweeps out on the sky, and so to the product of lens proper motion and angular Einstein radius. Each of these falls off with lens distance, so the signal is dominated by close lenses (within  $\sim 1$  kpc of the Sun). The all-sky source-averaged astrometric microlensing optical depth is  $\sim 10^{-5}$ , over an order of magnitude greater than the photometric microlensing optical depth [5]. Fig. 1 shows two views of an astrometric microlensing event. The upper panel shows the right ascension and declination recorded by a barycentric and a terrestrial observer (or equivalently a satellite at the  $L_2$  Lagrange point, like *GAIA*). However, *GAIA* does not provide the data in such a clean form. The observed quantity is the CCD transit time for the coordinate along the scan. (This is the same way that the *Hipparcos* satellite worked [6]). From the sequence of these

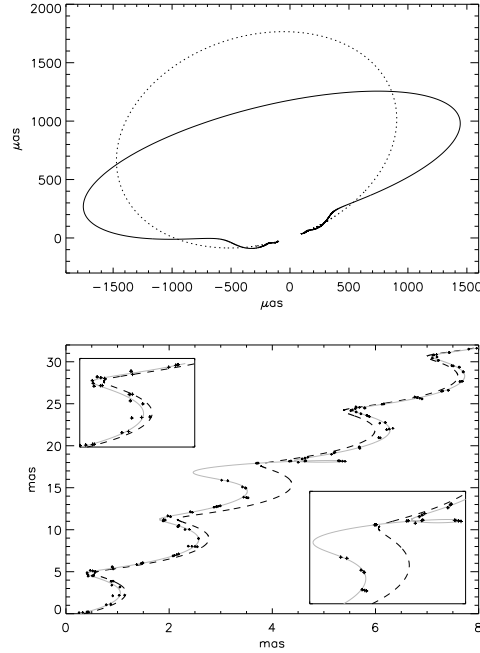


Figure 1: Upper panel: Astrometric shift of a microlensing event, as seen by a barycentric (dotted line) and a terrestrial observer (solid line). Lower panel: Simulated data incorporating typical sampling and astrometric errors for *GAIA*. Also shown for comparison are the theoretical trajectories of the source with (grey line) and without (dashed line) the event. The insets show the deviations at the beginning and the midpoint of this high signal-to-noise event. (The accuracy of the astrometry is  $300 \mu\text{as}$ , corresponding roughly to a 17th magnitude star).

one-dimensional measurements, the astrometric path of the source, together with any additional deflection caused by microlensing, must be recovered. The lower panel shows the event as seen by *GAIA*. The simulated datapoints have been produced by generating random transit angles, and sampling the astrometric curve according to *GAIA*'s scanning law. The transits are strongly clustered, as *GAIA* spins on its axis once every 3 hours and so may scan the same patch of sky four or five times a day. The transit angle is the same for all transits in such a cluster, but changes randomly from cluster to cluster. The two insets show the astrometric deviations at the beginning and at the maximum of the event, from which it is clear that *GAIA* can detect that a

microlensing event has occurred.

Can the local mass function be recovered from the astrometric microlensing signal seen by *GAIA*? A covariance error analysis shows that  $\sim 2500$  astrometric events detected by *GAIA* will be of such high quality that the mass of the lens will be recovered with good accuracy [5]. These events are biased towards lenses with mass greater than  $0.3M_{\odot}$ . This is not too surprising, as it is more difficult to measure the deviation if the Einstein radius is small. This already suggests that *GAIA*'s astrometric microlensing signal will be an unbiased and powerful probe of the local population of stellar remnants, such as white dwarfs and neutron stars. However, the signal seen on smaller mass-scales will require modelling and correction for selection effects before it is unbiased. Reid & Hawley [6] compute the mass function (MF) for nearby stars from the volume-limited *8 Parsec Sample* using empirical mass-luminosity relationships. They obtain a power-law MF ( $f(M) \propto M^{-1}$ ) over the range 0.1 to  $1.0M_{\odot}$ . This is in rough agreement with the MF as inferred from studies of the luminosity function (LF) of red disk stars seen with *Hubble Space Telescope* [7]. The behaviour of the MF becomes more uncertain as the hydrogen-burning limit is approached. So, we use three MFs that span the range of reasonable possibilities. Above  $0.5M_{\odot}$ , the MF is always derived from the Reid-Hawley luminosity function. Below  $0.5M_{\odot}$ , it may be flat ( $f(M) \propto M^{-1}$ ), rising ( $f(M) \propto M^{-1.44}$ ) or falling ( $f(M) \propto M^{0.05}$ ). For the falling MF, we choose the power-law index to be that implied by the decline in the LF below  $M_v \approx 13$ . For the rising MF, we choose the power-law index by assuming that the rise at  $M_v \approx 11$  continues to fainter magnitudes and that these stars are missing from the data because of incompleteness. Of course, the flat MF is so called because it has equal numbers of objects in each decade of mass and so appears flat in a plot of  $\log Mf(M)$  versus  $\log M$ . For each of the three MFs, we generate samples of 2500 astrometric microlensing events from models of the Galaxy and compute the mass uncertainty using the covariance analysis. (In actual practice, the high quality events would be selected on the basis of the goodness of their  $\chi^2$  fits). We build up the MF as a histogram. The vertical error bar associated with each bin is proportional to the square root of events in the bin. The horizontal error bar is the size of the bin.

The three cases are shown in Fig. 2 with the solid line representing the underlying MF. The simulated datapoints with error bars show the MFs reconstructed from the high quality events. It is evident that *GAIA* can easily distinguish between the flat, rising and falling MFs. The MFs are reproduced accurately above  $\sim 0.3M_{\odot}$ . Below this value, the reconstructed MFs fall below the true curves, as a consequence of the bias against smaller Einstein radii.

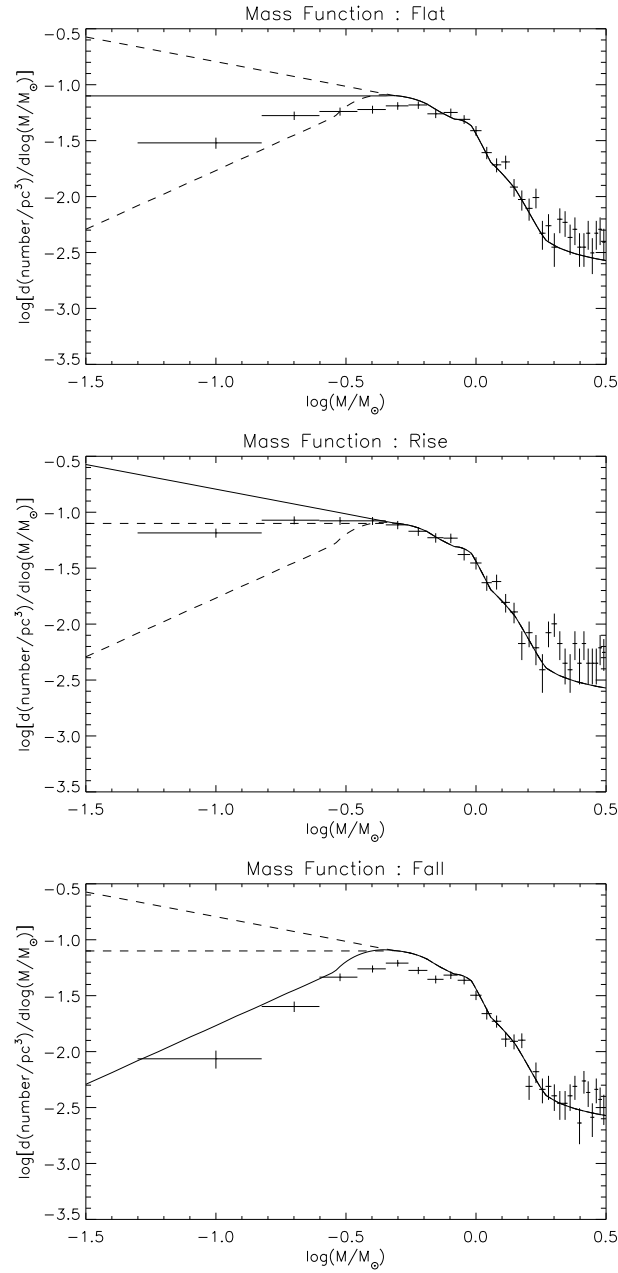


Figure 2: The recovery of the flat, rising and falling mass functions from the subsamples of high quality astrometric microlensing events generated from simulations. The vertical error bar associated with each bin is proportional to the square root of events in the bin. The horizontal error bar is the size of the bin.

However, this does not compromise *GAIA*'s ability to discriminate between the three possibilities. In practice, of course, simulations could be used to re-calibrate the derived MFs at low masses and correct for the bias. We have also carried out simulations with MFs containing spikes of compact objects, such as populations of  $\sim 0.5M_{\odot}$  white dwarfs. They lie in the mass régime to which *GAIA*'s astrometric microlensing signal is most sensitive. So, such spikes stand out very clearly in the reconstructed MFs. We conclude that one of the major scientific contributions that *GAIA* can make is to determine the local MF. Microlensing provides the only way of measuring the masses of individual objects irrespective of their luminosity. *GAIA* is quite simply the best survey instrument to carry out an inventory of masses in the solar neighbourhood.

### 3 Supernovae Detection

Supernovae (SNe) are divided into type I and II primarily on the basis of their spectra, with lightcurve shape as a secondary diagnostic. SNe Ia are thermonuclear explosions in white dwarf stars which have accreted too much matter from a companion. It is unclear whether the companion is also a white dwarf or is a main sequence/red giant star. In fact, whether the progenitors of SNe Ia are doubly degenerate or singly degenerate binaries is one of the major unsolved problems in the subject. SNe Ib/c and II originate in the core collapse of massive stars. SNe Ia have found ready application in cosmology. Their intrinsic brightness means that they can be detected to enormous distances. Although their peak luminosities vary by a factor of 10, Phillips [9] found a correlation between the peak absolute magnitude and the rate of decline, which enables SNe Ia to be calibrated and used as “standard candles”. Claims for an accelerating universe partly rest on their use as distance estimators, yet there are obvious concerns regarding systematic errors [10]. So, a major thrust of modern SNe studies is to understand and quantify the differences in the morphology of SNe Ia lightcurves and the scatter in the Phillips relation. *GAIA* is an ideal tool to study nearby SNe (within a redshift  $z \sim 0.14$ ). *GAIA* will provide a huge dataset of high quality local SNe Ia in which any deviations from “standard candles” can be analysed. Here, we ask the question: *How many supernovae will GAIA detect over the five-year mission lifetime?*

Richardson et al. [11] use the Asiago Supernova Catalogue to study the V band absolute magnitude distributions according to type. They find that the mean absolute magnitude of SNe Ia at maximum is  $-18.99$ . This figure

includes the contribution from the internal absorption of the host galaxy. As *GAIA*'s limiting magnitude is  $V \sim 20$ , this means that the most distant SNe Ia accessible to *GAIA* are  $\sim 630$  Mpc away. Similarly, the mean absolute magnitude of SNe Ib/c at maximum is  $-17.75$ , so that the most distant SNe Ib/c detectable by *GAIA* are  $\sim 355$  Mpc away. SNe II are subdivided further according to lightcurve into linear (L) and plateau (P) types. The mean absolute magnitude of II-L type is  $-17.63$  and of II-P type is  $-16.44$  (Richardson et al. 2002). These correspond to distances of  $\sim 335$  Mpc and  $\sim 195$  Mpc respectively. Such distances emphasise that *GAIA* is the ideal tool to discover relatively nearby SNe.

The rates with which SNe occur in different galaxies at low redshift are given in van den Bergh & Tammann [12]. The host galaxies follow the local large-scale structure. We use the latest version of the CfA redshift catalogue [13]. This contains the sky positions and heliocentric velocities of  $\sim 20\,000$  galaxies. On plotting numbers of galaxies versus distance, the graph peaks at  $\sim 75$  Mpc and thence shows a steady decline. This suggests that the CfA catalogue can be used out to at most  $\sim 75$  Mpc. The numbers in the catalogue must be regarded as lower limits to the true numbers within 75 Mpc, as the luminosity functions (LFs) derived from the catalogue are incomplete at faint magnitudes. Beyond 75 Mpc, we assume that the distribution of galaxies is homogeneous and that the number scales like  $D^3$  where  $D$  is the heliocentric distance. Given the numbers of galaxies and the observed rates, we can then straightforwardly compute the total number of SNe that explode during the five-year *GAIA* mission lifetime and are brighter than the limiting magnitude. In all, there are at least  $\sim 48\,000$  SNe Ia and  $\sim 7\,000$  SNe Ib/c. The numbers for SNe II depend on the relative frequency of II-L with respect to II-P, which is not very well-known. Henceforth, we denote the fraction of all SNe II that are L-type by  $f_{II}$ . Then, the numbers of SNe II that explode are  $\sim 28\,500f_{II} + 5\,600(1 - f_{II})$ . These numbers are lower limits for two reasons – first because no contribution from faint galaxies is included and second because *GAIA*'s limiting magnitude may be deeper than 20th in practice.

By using simulations of SNe detection with *GAIA*'s scanning law [14], we find that *GAIA* records data on 30% of all the SNe Ia within 630 Mpc, which marks the limit of the most distant SNe Ia accessible. Similarly, *GAIA* records data on  $\sim 20\%$  of all SNe Ib/c,  $\sim 31\%$  of all SNe II-L and  $\sim 48\%$  SNe II-P within these distances. This means that *GAIA* will provide some (perhaps rather limited) information on 14 300 SNe Ia and 1400 SNe Ib/c during its five-year mission. For SNe II, the number depends on the relative frequency  $f_{II}$  and is  $\sim 8\,700f_{II} + 2\,700(1 - f_{II})$ . If SNe II-L and SNe II-P occur equally

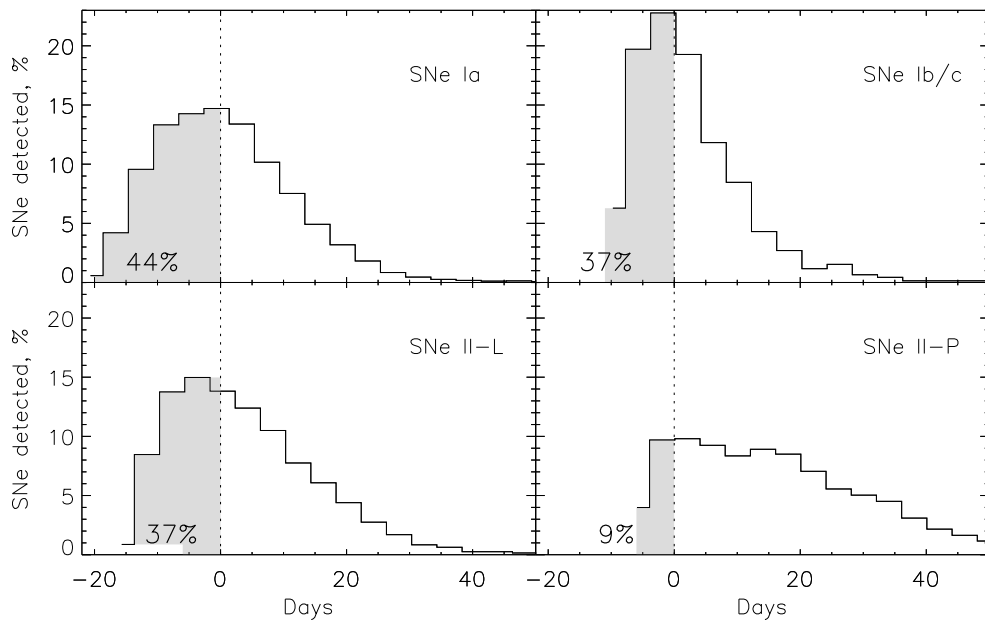


Figure 3: This shows histograms of the numbers of detected SNe against phase of the lightcurve. The shaded area corresponds to the fraction of SNe caught before the maximum of the lightcurve.



frequently ( $f_{II} = 0.5$ ), then the total number of SNe II is  $\sim 5700$ . In other words, *GAIA* will provide some information on  $\sim 21\,400$  SNe in total. These are huge numbers, both compared to the sizes of existing catalogues and to the likely datasets gathered by other planned space missions. Almost all the SNe that *GAIA* misses explode in the 20 days just after *GAIA* samples that location in the sky. Before the next transit of the telescopes, the SN reaches maximum and then fades to below *GAIA*'s limiting magnitude ( $V \sim 20$ ).

Fig. 3 shows the fraction of the detected SNe as a function of phase of the lightcurve. Some 44% of the detected SNe Ia are caught before maximum, 37% of the detected SNe Ib/c, 37% of the detected SNe II-L and 9% of the detected SNe II-P. The low fraction for SNe II-L is largely a consequence of the fact that they are intrinsically the faintest. The total number of all SNe found before maximum during the 5 year mission lifetime is  $\sim 8\,500$ . This number can be broken down into  $\sim 6\,300$  SNe Ia,  $\sim 500$  SNe Ib/c and 1700 SNe II (assuming  $f_{II} = 0.5$ ).

*GAIA* will provide a large dataset of nearby SNe, which are very interesting from the point of view of understanding the properties and the underlying physics of the explosions themselves. The advantage of SNe surveys with *GAIA* is that selection effects are either minimised or easy to model, and that there will be many examples of comparatively scarce phenomena (e.g., subluminous SNe, SNe II-L, SNe Ib/c). At present, SNe rates come from relatively small datasets and are subject to substantial uncertainties. Selection effects – depending on the type of host galaxy, the extinction and the distance from the center of the galaxy – seriously afflict all current datasets. Given the large numbers of alerted SNe, *GAIA* will provide accurate rates as a function of position, extinction and type of host galaxy. These give valuable, if indirect, information on both the star formation rate and the high mass end of the mass function. There have also been suggestions that populations of subluminous SNe may have been systematically missed in existing catalogues [11]. If so, then *GAIA* is the ideal instrument with which to find them.

## 4 Conclusions

The *GAIA* satellite is scheduled for launch in about 2010. It will determine the positions, velocities and astrophysical nature of over a billion stars distributed throughout the Milky Way Galaxy and into the Local Group. Each object will be monitored between 150 and 400 times during the 5 year mission (depending on ecliptic latitude). The resulting catalogue will be one of the largest astro-

physical datasets ever taken. The positions and velocities of stars, together with the changing brightness of variable sources (e.g., bursting and eruptive stars, supernovae, killer asteroids, eclipsing variables, microlensed stars), will all be synthesized into a three-dimensional movie show.

This article has discussed two applications of real-time detection of variable sources with the *GAIA* satellite. *GAIA* will provide the best determination of the local mass function of stars down to brown dwarf mass scales – which is important for reckoning the baryonic and particle dark matter content of the solar neighbourhood. This can be inferred from the astrometric microlensing signal of nearby stars. *GAIA* will provide the largest sample of nearby supernovae ever acquired – which is crucial for assessing how the scatter in properties affects their use as cosmological distance indicators. This will provide opportunities both for follow-ups in other wavebands (e.g., X ray and gamma-ray) and with other detectors (e.g., neutrino, gravitational waves). Further applications are given in references [5] and [14].

- [1] H. Kraus, 2000, In “IDM 2000: The Identification of Dark Matter”, eds N. Spooner, V. Kudryavtsev (World Scientific: Singapore), p. 275
- [2] K. Kuijken, G. Gilmore, 1991, ApJ, 367, L9; J.J. Binney, N.W. Evans, 2001, MNRAS, 327, L27
- [3] M.A. Strauss et al. 1999, ApJ, 522, L61; A.J. Burgasser et al. 2000, AJ, 120, 1100; J.E. Gizis, J.D. Kirkpatrick, J.C. Wilson, 2001, AJ, 121, 2185
- [4] M.A. Walker, 1995, ApJ, 453, 73; E. Høg, I.D. Novikov, A.G. Polnarev 1995, A&A, 294, 287; J. Miralda-Escudé 1996, ApJ, 470, L113
- [5] V.A. Belokurov, N.W. Evans, 2002, MNRAS, 331, 649
- [6] ESA 1997, The Hipparcos and Tycho Catalogues, ESA SP-1200 (ESA Publications: Noordwijk)
- [7] I.N. Reid, S. Hawley, 2000, New Light on Dark Stars (Springer Verlag: New York), chaps 7, 8.
- [8] A. Gould, J.N. Bahcall, C. Flynn, 1997, ApJ, 482, 913
- [9] M.M. Phillips, 1993, ApJ, 413, L105

- [10] B. Leibundgut, 2000, *A&A Rev.*, 10, 179; B. Leibundgut, 2001, *ARAA*, 39, 67
- [11] D. Richardson, D. Branch, D. Casebeer, J. Millard, R.C. Thomas, E. Baron, 2002, *AJ*, 123, 745.
- [12] S. van den Bergh, G.A. Tammann, 1991, *ARAA*, 29, 363.
- [13] J. Huchra, M. Geller, C. Clemens, S. Tokarz, A. Michel 1992, *Bull. Inf. C.D.S.* 41, 31
- [14] V. Belokurov, N.W. Evans 2001, *MNRAS*, in press ([astro-ph/0210570](#)).